JOURNAL OF MATERIALS SCIENCE **37** (2002) 4019–4028

Electrophoretic deposition of alkaline earth coatings from EDTA complexes

S. N. B. HODGSON, X. SHEN
Institute of Polymer Technology and Materials Engineering, Loughborough University, Loughborough, Leicestershire, LE11 3TU, UK
E-mail: S.N.B.Hodgson@Lboro.ac.uk

F. R. SALE
Manchester Materials Science Centre, University of Manchester and UMIST, Manchester, UK

A novel process route combining electrophoretic deposition (EPD) and ethylene-diamine-tetra-acetic acid (EDTA) complexation has been developed and used to produce crack-free coatings of alkaline earth oxides with thickness up to 8 μm after heat treatment at 700°C. Aqueous systems were found to be unsuitable for the EPD process due to their high conductivity and the effect of liberated gas evolved on the electrodes, and a non-aqueous based alternative formulation was developed based on methanol (solvent/carrier) and ethanediol (stabiliser) in conjunction with the EDTA complexes to allow the EPD process to be successfully used to deposit porous coatings. The coating process has been investigated by electrochemical impedance spectroscopy (EIS), and is thought to involve a combination of the migration of complexed ions in solution, their precipitation as charged colloidal particles in the vicinity of the anode, followed by their aggregation at, and adhesion to the anode surface. It is believed the process may have application for the low cost deposition of a wide range of porous coatings.

1. Introduction

The alkaline earth oxides, particularly BaO, SrO and BaSrO solid solutions have application both individually and as a constituent of a range of functional and chemical applications, including energy conversion, catalysis [1, 2] and electron emission [3]. Generally the processing requirements of these materials are that they can be produced in a stable, surface-active form, typically as porous coatings or thin films.

Electrophoretic deposition (EPD) is an established technique based on a phenomenon associated with the movement (electrophoresis) and deposition of colloidal particles suspended in an aqueous or a non-aqueous medium under an electrical field [4]. In recent years, this technique has attracted renewed interest for application in the production of ceramic coatings due to a range of potential advantages over competing processes such as dip-coating and spraying, including the possibility of producing uniform thickness coatings on complex shaped products, with greater thickness and higher process rates [5]. The deposition process during EPD remains the subject of some debate, although several mechanisms have been proposed, notably, discharge of charged particles at the electrode surface, polymerisation of adsorbed hydroxides produced by secondary processes at the depositing electrode and more recently distortion and subsequent thinning of the double layer lyosphere by the electric field particle coagulation due to local electrolyte concentration increase caused by electrochemical reactions [4, 6].

Sol-gel techniques including those based on alkoxide precursors and aqueous colloids have attracted much interest for the preparation of thin coatings. However, the thickness of such coatings is typically limited to <1 μm, for single process cycles. Attempts to develop electrophoretic deposition for use directly in combination with the alkoxide and/or aqueous sol-gel processes to produce thicker coatings have been made, particularly for silica based systems, but have been of only partial success primarily due to the large shrinkage stresses generated on drying and sintering of these materials, which results in cracking [7]. In addition there are also significant issues regarding the cost, stability and control over particle size where such an approach is extended to oxides other than silica.

In contrast aqueous organic complex routes such as citrate and EDTA gel processes, which involve the formation of stable metal complexes in solution, and which can form a range of gel or particulate type products on dehydration might offer a viable alternative process as a precursor to EPD deposition for a wide range of compositions, provided the substrate is compatible with the somewhat higher process temperatures used during the thermal conversion of the gel products to the oxides in comparison with direct routes to the oxide such as sol-gel. However, little or no information exists regarding EPD of such materials.

There are some significant differences between the nature of the coating process involving these precursors and more conventional EPD processes based on

colloidal oxide suspensions. Most important amongst these is that the coatings which are deposited by this process comprise not the oxide directly, but rather oxide precursors in the form of organic complexes of the metal ions which are subsequently thermally decomposed to the oxide form via a multi stage decomposition process, with substantial mass and volume reductions [8].

The precursor used in this work comprised solutions of the barium and strontium nitrates complexed with Ethylene Diamine Tetra Acetic Acid [EDTA = $(CH_2N)_2(CH_2COOH)_4$]. The complexing reactions for these metal ions are of the form:

$$M^{2+} + Y^{4-} \Leftrightarrow MY^{2-} \quad (1)$$

Where

$$Y^{4-} = (CH_2N)_2(CH_2COO)_4^{4-}$$

The resultant complexes, which form in aqueous solution under appropriate conditions interact with increasing concentration to form aqueous organic gels which undergo multiple stage decompositions with increasing temperature to yield the corresponding oxides, typically at temperatures below 1000°C [8].

Typically the changes occurring on heat treatment of such EDTA complexes involve a three stage process, of dehydration at temperatures up to approximately 200°C, a second stage of breakdown of the gel, accompanied by softening/melting in the range approximately 200–400°C, and thermal decomposition and combustion of residual semi-organic materials to form the carbonate and/or oxide phases temperatures above approximately 400°C [8–10].

The equilibrium constant for the reaction shown in Equation 1 is dependent upon the pH of the solution. At high pH the formation of the Y^{4-} ions from EDTA is enhanced, together with the formation of the complexed MY^{2-} species [8, 11]. The additions of ammonia used in this process are required both to facilitate the dissolution of the EDTA, and also to raise the pH to a point at which the extent of complexation is sufficient to allow stable solutions and gels to be formed. A pH of 6 was found to be sufficient to facilitate this for the barium and strontium nitrate derived systems used in this work.

2. Experimental procedure

2.1. Preparation of the coating sol

The starting reagents used were AnalaR grade $Ba(NO_3)_2$, $Sr(NO_3)_2$, EDTA, 35% ammonia solution and ethanediol (99%) supplied by BDH and Fisons, respectively. The alkaline earth-EDTA sol ($[Ba_{0.5}Sr_{0.5}]$-EDTA sol) was prepared as described in detail in a separate publication [8], by mixing 0.1 M solutions of the nitrate precursors with 0.1 M solutions of EDTA, using ammonia additions to control the pH at a value of 6. The resultant solution then was dehydrated in a rotary evaporator under a vacuum at 60–70°C to produce a viscous liquid (2 M aqueous solution of $[Ba_{0.5}Sr_{0.5}]$-EDTA). Final additions of ammonia solution were made to adjust the pH to a value of 6. Solid samples for FTIR and thermal analysis were obtained by further dehydration of this aqueous solution in a vacuum oven at 80°C for 10 hours.

Investigations were performed into the use of the aqueous solution and colloidal sol obtained from these precursors directly for EPD, together with a range of primarily nonaqueous systems prepared by making 10 vol% additions of this 2 M aqueous $[Ba_{0.5}Sr_{0.5}]$-EDTA solution to appropriate organic media. The range of nonaqueous media investigated included ethanol, ethanol-ethanediol, methanol and methanol-ethanediol, with the additions being made at room temperature and with continuous stirring in each case. The use of these predominantly non-aqueous media precluded the measurement of pH in a reliable form in these systems.

2.2. Electropheretic deposition and characterisation of the coatings

The EPD was carried out on the anode of a triple electrode cell. The system used for these investigations comprised 80 vol% methanol; 10 vol% ethanediol; and 10 vol% of the 2 Molar $[Ba_{0.5}Sr_{0.5}]$-EDTA solution prepared as described above. A DC power supply (PL320) was used, at a range of fixed deposition voltages between 1 and 5 Volts, with the deposition current and voltage recorded as a function of time. Nickel foil obtained from Philips Components (UK) was used as the electrodes. The distance between the anode and cathodes was 18 mm with an electrode area of 140 mm^2.

In order to improve the wettability and coating adhesion, a standard cleaning and pre-treatment process was used. The nickel foil was first degreased in acetone for about 2 minutes at room temperature and then etched in a 50 vol% solution of glacial acetic acid in acetone for 5 minutes at room temperature, washed in deionised water followed by an acetone rinse and dried in air at room temperature.

Following completion of the EPD process, the coated electrode was carefully removed from the liquid, with the coating initially dried in air at room temperature for 10 hours and then dried further in a vacuum oven at 80°C for 5 hours. The dried gel coating was then heat-treated in a tube furnace at 700°C for 1 hour, with a heating rate of 10°C/min, under a reduced pressure of about 100 Pa. The heat treatment temperature of 700°C was determined on the basis of thermal analysis studies of the alkaline earth-EDTA gels [8], with this temperature being sufficient to allow thermal decomposition of the gel products whilst limiting any surface oxidation of the nickel substrate under this reduced pressure.

2.3. Impedance spectroscopy

Electrochemical impedance spectroscopy (EIS) was used to investigate the electrophoretic deposition processes in the methanol-ethanediol-$[Ba_{0.5}Sr_{0.5}]$-EDTA system as used for the EPD studies. An electrochemical cell consisting of a working electrode made of the nickel foil described in the previous section, with a surface area of 160 mm^2 in the suspension and a graphite counter electrode with a diameter of 5 mm with a surface area of approximately 390 mm^2 in the suspension, was used as a combined analytical and electrophoresis cell for these experiments. The distance between the working electrode and the counter electrode was 10 mm. A computer controlled potentiostat

(ACM Instrument model Gill AC) was used to measure the impedance of the various specimens. An alternating current (AC) signal of maximum amplitude 64 mV and direct current (DC) polarisation signal of 1000 mV were used over a frequency range between 0.05 to 30,000 Hz. 40 points were collected automatically for each measurement. The results were then analysed using commercial software (EIS Analysis) to determine the complex impedance diagram and model an equivalent electrical circuit in terms of the resistive, capacitive and impedance elements which would produce an analogous electrical response.

2.4. Characterisation

The composition of the as-prepared coating sols was studied by Fourier Transform InfraRed Spectroscopy (FTIR) using a Mattson3000 FTIR spectrometer. Particles of the alkaline earth-EDTA complexes formed on dehydration of the sol were investigated by transmission electron microscopy. A JEOL-JEM100 instrument was used, using a carbon film to support the particles.

The decomposition process of the gel was investigated by thermo-gravimetric analysis (TGA) and differential scanning calorimetry (DSC), with a heating rate of 10°C/minute in air. The morphology and cross-section thickness of coatings were examined both prior to and after heat treatment by Scanning Electron Microscopy (SEM). Samples were gold-coated to reduce charging effects, with specimens for cross-sectional analysis being prepared by mounting in epoxy resin (SpeciFix-20), followed by normal grinding, polishing procedures.

3. Results and discussion

3.1. EDTA complex formation and thermal decomposition

The FTIR spectra for the $[Ba_{0.5}Sr_{0.5}]$-EDTA and $[Ba_{0.5}Sr_{0.5}]$-EDTA-ethanediol systems are shown in Fig. 1 together with the equivalent spectra of the uncomplexed EDTA and ethanediol. The wavenumber shift from 1695 cm^{-1} in the uncomplexed EDTA (due to C=O stretching) to 1614 cm^{-1} is indicative of the formation of alkaline earth-EDTA complexes. In the presence of ethanediol this peak shifted to higher wavenumber 1626 cm^{-1}. This can be attributed to an increase in the covalent bonding character and hence bond strength of the chelating bonds in these complexes [10].

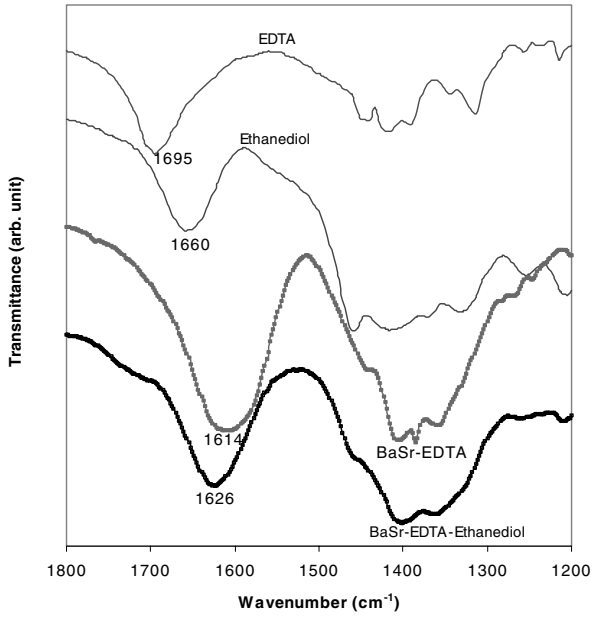

Figure 1 The effect of formation of the alkaline earth-EDTA complexes on FTIR spectra without and with ethanediol.

3.2. Particle formation from EDTA complexes

In many ways, the EDTA complexes used as precursors in this work are quite different from the particulate suspensions used in conventional EPD.

It would be anticipated that the complexed metal ions would be present in the form of a solution in these aqueous and mixed aqueous organic systems. However, as shown in Fig. 2, dehydration of these solutions results in the precipitation of fine particles of the metal-organic gel complex, with particle size in the range 1–20 nm. A typical FTIR spectra of these products is shown in Fig. 1. The sequence of events corresponding to gradually increased concentration on dehydration is thus as follows:

$$MY^{2-} \text{ Complexes in solution} \rightarrow \text{colloidal sol} \rightarrow \text{gel}$$

The gelation effect obtained on dehydration of these aqueous systems in bulk conditions can be attributed to the fine particle size in these intermediate "sols".

The coatings obtained from the EPD of these systems appear chemically and structurally similar to the material obtained on dehydration of bulk sols, and although it is difficult to experimentally verify, it is probable that a similar sequence of events to that accompanying dehydration occurs locally at the electrode surface. It would be anticipated that the transport of the charged complexes to the electrode results in a localised increase in concentration of these species. By analogy with the effect of concentration increase from dehydration of these systems described above, this would be expected to result in the formation of colloidal particles, as an intermediate stage in the deposition process, with these being subsequently deposited on the electrode. The process, which is schematically illustrated in Fig. 3, can thus be defined as a form of electrophoretic deposition.

3.3. Thermal analysis of coating decomposition and conversion to oxide

The mass changes occurring during heat treatment and thermal decomposition of the gel samples obtained from the aqueous based $[Ba_{0.5}Sr_{0.5}]$-EDTA and the organic based methanol-ethanediol-$[Ba_{0.5}Sr_{0.5}]$-EDTA system are shown in Fig. 4. The thermal decomposition behaviour of this gel was described in detail in elsewhere [8]. The decomposition process observed from these samples is generally typical for the decomposition of EDTA complexes [9, 10], and essentially comprises three stages: (i) dehydration between 50–200°C; (ii) a first decomposition between 200–400°C associated with the initial break-down of the metal-EDTA complexes and liberation of H_2O, CO_2 and NO_2; (iii) a second decomposition between 400–550°C related to

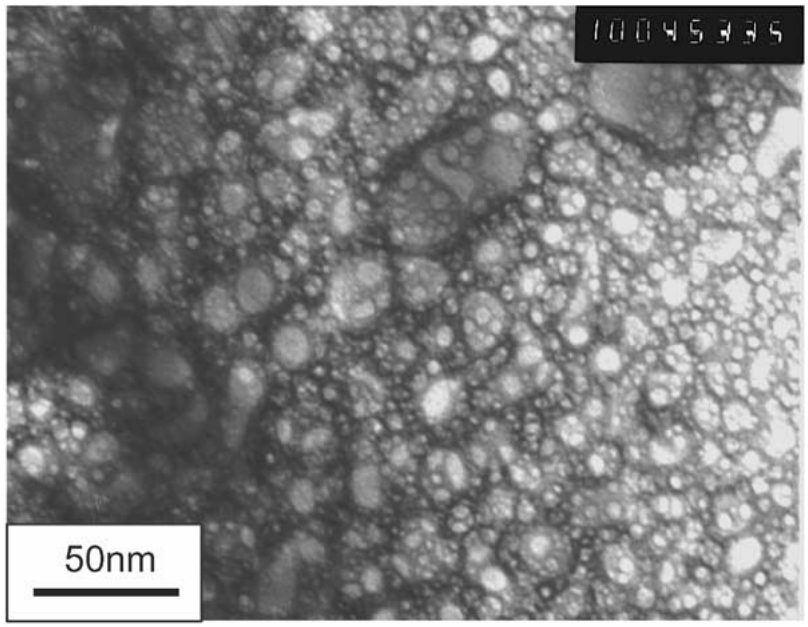

Figure 2 TEM micrograph of the particles formed on dehydration of the $[Ba_{0.5}Sr_{0.5}]$-EDTA sol.

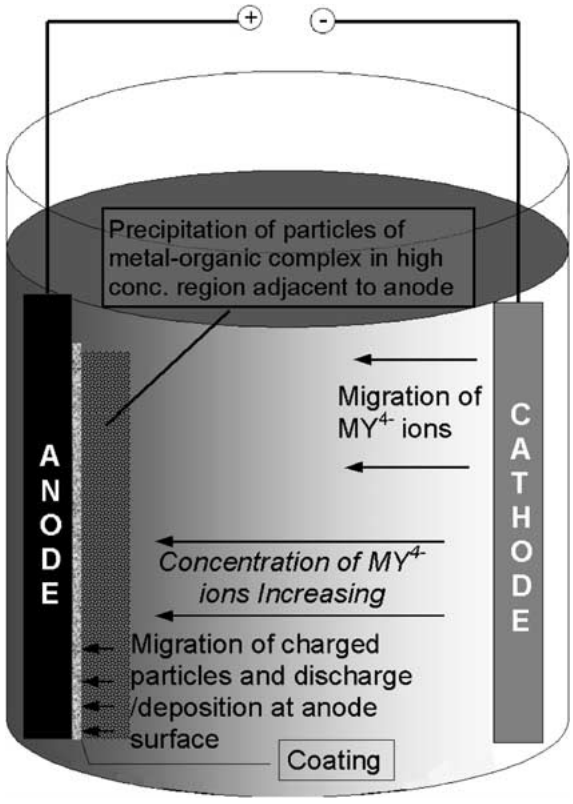

Figure 3 Processes occurring during electrophoretic deposition of coating from solution containing metal-EDTA complexes.

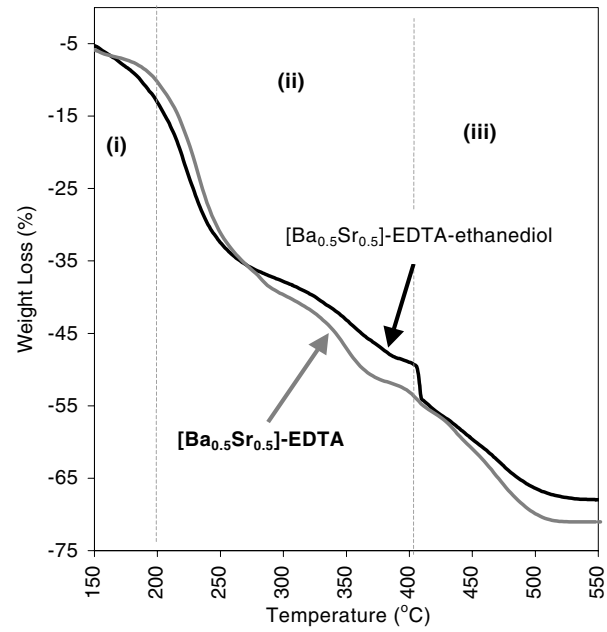

Figure 4 TG results showing the decomposition of $[Ba_{0.5}Sr_{0.5}]$-EDTA gel with and without ethanediol addition.

the oxidation and decomposition of the residual organic substances.

Our previous work has shown that the solid product of the (stage (iii)) decomposition of $[Ba_{0.5}Sr_{0.5}]$-EDTA gel for temperatures up to 700°C is the alkaline earth carbonate solid solution $[Ba_{0.5}Sr_{0.5}]CO_3$, which can be converted to an oxide solid solution at higher temperatures [8]. These results indicate very similar behaviour for the decomposition of the gel complexes with ethanediol addition, but with significantly reduced decomposition at temperatures up to approximately 400°C and the transition temperature between the stage (ii) and stage (ii) decomposition increased from approximately 350°C without ethanediol to approximately 400°C with ethanediol addition. Such an effect would be consistent with an increase in the strength of the chelating bonds in the complex, as discussed for the FTIR results, and increased stability against the thermal breakdown of the complex. The mechanism responsible for this enhanced stability in the presence of ethanediol additions is not fully understood at this time.

3.4. Coating production by EPD

3.4.1. Development of coating sols

A range of tests on the coating formation were carried out to determine the optimum deposition potential and dispersant for the EPD process.

TABLE I Properties of various organic based EDTA sol systems as investigated for electrophoretic deposition

Composition of solution (v%)	Approx. viscosity	Period of stability
Ethanol + $[Ba_{0.5}Sr_{0.5}]$-EDTA sol (1)	0.7 cp	2 seconds
Ethanol + ethanediol (10) + $[Ba_{0.5}Sr_{0.5}]$-EDTA sol (1)	1.4 cp	3 minutes
Methanol + $[Ba_{0.5}Sr_{0.5}]$-EDTA sol (20)	0.7 cp	30 minutes
Methanol + ethanediol (5) + $[Ba_{0.5}Sr_{0.5}]$-EDTA sol (15)	1.3 cp	120 minutes
Methanol + ethanediol (10) + $[Ba_{0.5}Sr_{0.5}]$-EDTA sol (10)	1.9 cp	180 minutes
Methanol + ethanediol (10) + $[Ba_{0.5}Sr_{0.5}]$-EDTA sol (15)	2.0 cp	150 minutes
Methanol + ethanediol (10) + $[Ba_{0.5}Sr_{0.5}]$-EDTA sol (20)	2.0 cp	110 minutes

Attempts to directly utilise the aqueous EDTA solution prepared as described in Section 2.1 were of limited success due to the effects of gas bubbles generated at the electrodes, which prevented effective coating formation. This bubbling phenomenon, arising from the electrolysis of the water increased with increasing deposition voltage. It is thought that the enhanced conductivity of the water due to the presence of the EDTA ions in solution exacerbated this effect.

The dispersion of the aqueous EDTA sol in an organic carrier was investigated as a method to reduce the liquid conductivity and hence the problems of electrolysis. However, dilution of the aqueous sol in a range of organic liquids was found to generally result in instability of the resultant system and rapid precipitation of agglomerated particles, as shown in Table I. The addition of ethanediol was found to reduce this precipitation and agglomeration of particles and hence stabilise the system. This increased stability of the complex is consistent with increased bond strength of the complexing species in the presence of ethanediol as evidenced by the FTIR results shown in Fig. 1, and the enhanced thermal stability shown in Fig. 4.

Typically a system for EPD is required to exhibit; good chemical and physical stability against sedimentation, low viscosity to facilitate particle mobility and rapid deposition, and low conductivity to avoid liquid electrolysis. The optimum composition of the suspension for electrophoretic deposition was determined as (80 vol%) methanol—(10 vol%) ethanediol—(10 vol%) 2 M $[Ba_{0.5}Sr_{0.5}]$-EDTA solution on the basis of the stability, viscosity and the suppression of deleterious gas evolution at the electrodes. Methanol additions did successfully prevent liquid electrolysis but reduced the sol stability, whilst ethanediol provided good stability, but increased the viscosity significantly. The above composition provided a reasonable compromise between these parameters with the properties and behaviour of the various compositions summarised in Table I.

3.4.2. Coating preparation by EPD

Crack-free coatings with thickness up to 8 μm after heat treatment were successfully produced by EPD from the solution of composition (80 vol%) methanol—(10 vol%) ethanediol—(10 vol%) 2 M aqueous $[Ba_{0.5}Sr_{0.5}]$-EDTA as shown in Fig. 5a and b. However, the successful production of such coatings was found to be dependent on the deposition conditions used.

It was found that the rate of deposition from this solution on the nickel anode was minimal when the applied voltage was below 2.0 V, whilst the deposit formed was poorly adherent when the applied voltage was above 4.5 V with the suspension. A uniform deposit was formed on the anode with an applied voltage of 3.5 V. The maximum voltage was determined by the secondary electrode reactions [12], in which the water present in this organically modified suspension underwent electrolysis as described for the aqueous system. The quantity of evolved O_2 gas from the anode reaction above approximately 3.5 V appeared to expel the deposit away from the anode and resulted in gradually deteriorating coating quality and adherence. The applied voltage for the coating was thus a compromise to get a reasonable deposition rate and obtain good coating quality by limiting the gas production. Observation of the coating solution during deposition revealed that, particularly at high deposition voltages, particle precipitation and coagulation could be observed both at the anode surface and in the immediately adjacent volume of solution. This is consistent with the mechanism of coating formation proposed in Section 3.2.

Initially, the appearance of the coatings was dense and transparent, with these "gel" type coatings appearing featureless under SEM. However, on heat treatment at 700°C in air for 60 minutes, these systems underwent a transformation to a porous particulate structure, comprising particles of approximately 0.1 μm in diameter. The coatings also underwent significant shrinkage, typically from around 32 μm for the green coating to 8 μm after heat treatment, corresponding to a linear shrinkage of 75%.

In conventional particulate ceramic materials deposited by EPD or similar coating techniques, such a volume shrinkage would inevitably result in the delamination and failure of the coatings. However in the present case, thermal decomposition is accompanied by softening and melting of the gel complex, as evidenced by the endotherm shown by DSC analysis of the material (Fig. 6). It is believed that this softening and melting of the complex provides a mechanism of stress relief and allows the coatings to remain intact despite the large volume changes associated with the decomposition process. The porous nature of the coatings formed in this case is a requirement for their use in functional applications such as electron emission or catalysis.

The relationship between the deposition current, deposition time and thickness of the deposited coating from the suspension of methanol-ethanediol (10 v%)-$[Ba_{0.5}Sr_{0.5}]$-EDTA sol (10 v%) is shown in Fig. 7, for an applied constant voltage of 3.5 V. This

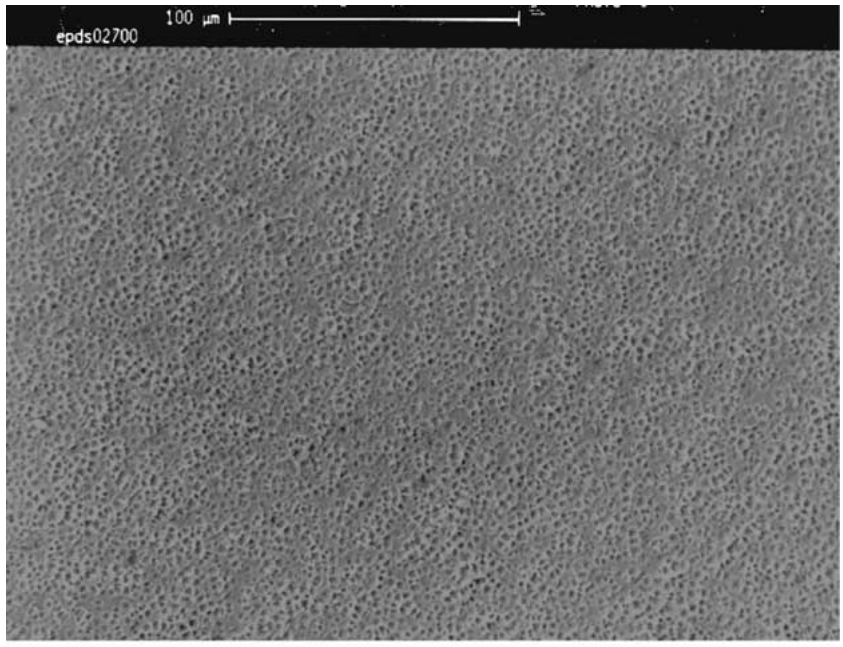

(a)

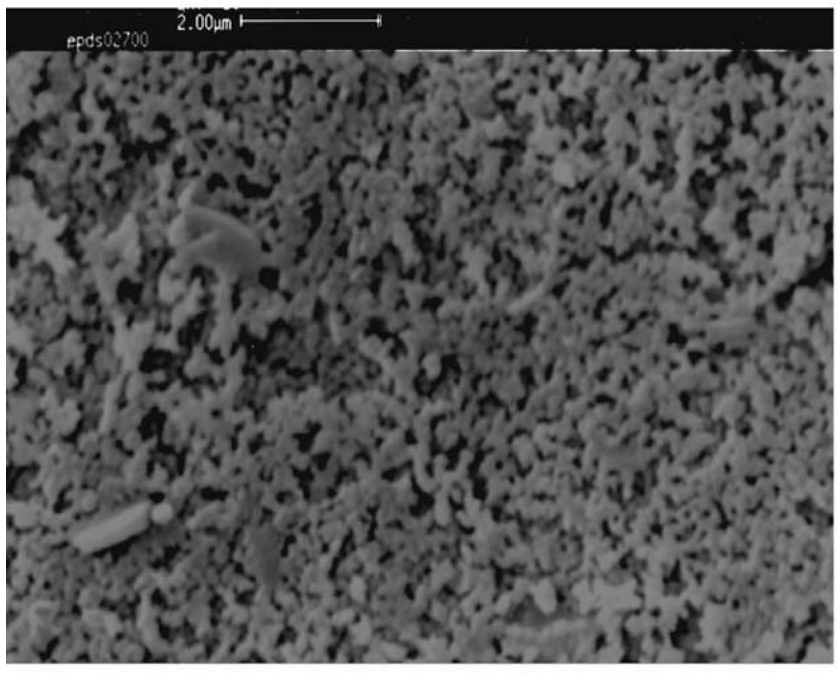

(b)

Figure 5 (a) Low and (b) high magnification SEM images of the coating prepared by EPD at a constant voltage of 3.5 V from (80 vol%) methanol—(10 vol%) ethanediol—(10 vol%) 2 M aqueous $[Ba_{0.5}Sr_{0.5}]$-EDTA, after heat treatment at 700°C for 60 minutes.

result confirms that appreciable rates of coating formation could be obtained for this applied voltage and composition. The decrease in the deposition current and deposition rate with time is due to an increase in the resistance between the two electrodes arising from the deposit formation on the anode. The change in the conducting behaviour of the suspension can be considered trivial due to the relatively small amount of the colloidal particles formed on the electrode in comparison to the total quantities of the EDTA complexes present in solution. As would be anticipated, the coating thickness increased with the deposition time. Attempts to produce and measure coatings above approximately 60 μm thickness were hampered by problems of poor adhesion and the subsequent displacement of the coatings as attempts were made to remove the coated electrodes from the liquid.

3.5. Study on the coating process by electrochemical impedance spectroscopy (EIS)

Although the theory of EIS has been largely developed for the study of corrosion processes and other redox reactions [13, 14], it was postulated that the method might be applicable to the electrophoretic deposition

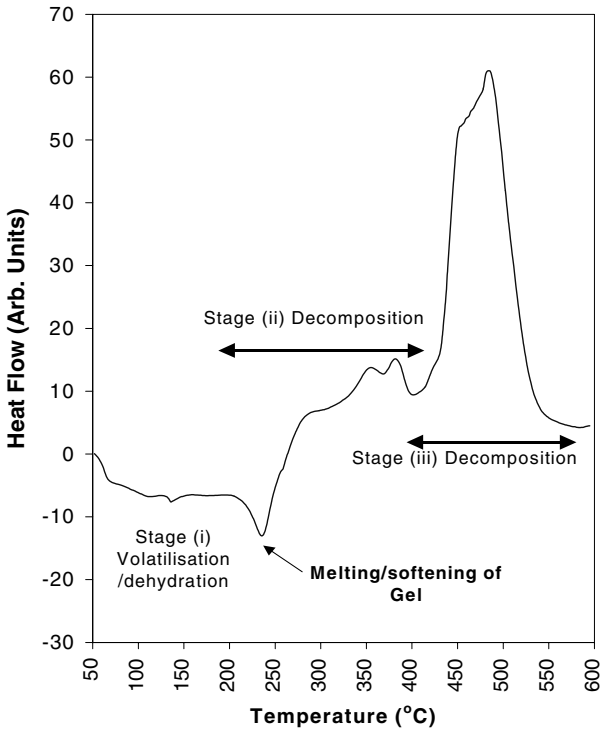

Figure 6 DSC investigation of effect of heat treatment on the $[Ba_{0.5}Sr_{0.5}]$-EDTA gel, indicating the softening melting phenomena associated with breakdown of the complex.

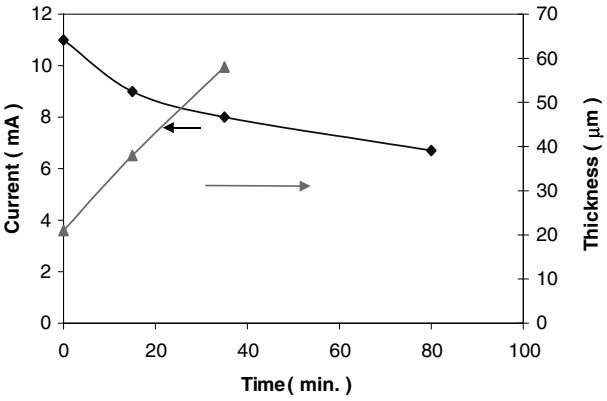

Figure 7 Relationship between deposition current, (as deposited) coating thickness and deposition time during the formation of the coating by electrophoretic deposition from (80 vol%) methanol—(10 vol%) ethanediol—(10 vol%) 2 M aqueous $[Ba_{0.5}Sr_{0.5}]$-EDTA, at a constant 3.5 volts.

process used in this study, where the charged complex species and neutralised or coagulated particles can be regarded as the reactant and product in the redox reaction, respectively. On the basis of this assumption, the established principles for evaluation of kinetic parameters such as electrolyte resistance R_Ω, charge-transfer resistance R_{ct}, electrical double layer capacitor C_{dl}, and Warburg impedance coefficient σ from the complex impedance diagram could be extended to analyse this process. However characterisation of such systems and coatings represents a new application for the technique and the findings must necessarily be regarded as tentative at this stage.

The complex impedance diagrams shown in Figs 8, 9, 11 and 12 comprise a plot of the real (Z') and Imaginary (Z'') components of the impedance of the EPD

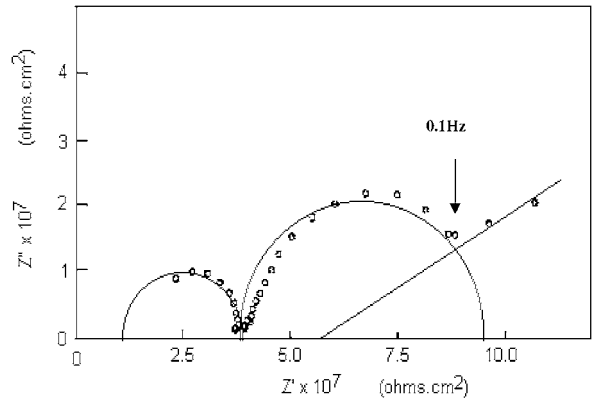

Figure 8 The complex impedance diagram obtained for the methanol used as an organic carrier/solvent in this work.

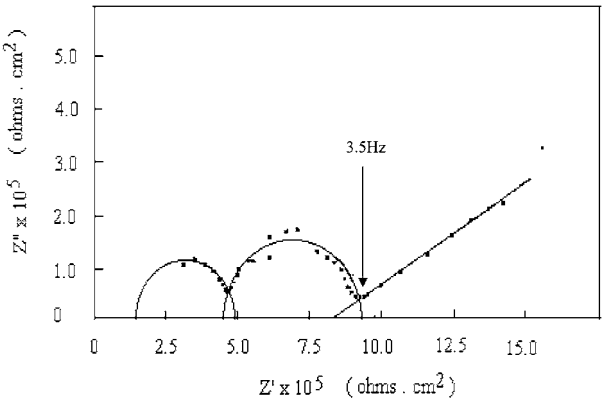

Figure 9 The complex impedance diagram obtained from the (80 vol%) methanol—(10 vol%) ethanediol—(10 vol%) 2 M aqueous $[Ba_{0.5}Sr_{0.5}]$-EDTA system used for EPD.

system. Each plot represents a sequence of measurements corresponding to increasing AC frequency moving from top right to bottom left. Typically, such plots comprise two regimes of behaviour. At low AC frequencies the electrical behaviour is dominated by diffusion of the charge carriers, whilst at higher measuring frequencies, charge transfer reactions become the dominant and limiting factor. These correspond respectively to linear and semicircular regions in the complex impedance diagrams. Such "ideal" behaviour is normally modelled in terms of the "Randles Equivalent Circuit" [13].

For simplicity, the voltage conditions used in this case were below the theoretical "break-down voltage" for electrolysis of water in order that complications arising from these additional electrode reactions were avoided. The complex impedance diagrams obtained from EIS investigation of the methanol–ethanediol-$[Ba_{0.5}Sr_{0.5}]$-EDTA sol, together with that obtained for methanol under equivalent conditions are shown in Figs 8 and 9 respectively.

From these figures it can be seen that the appearance of the complex impedance plots was broadly similar in each case. The two semicircles and the straight line observed in the diagram can not be interpreted on the basis of the Randles equivalent circuit for the simple redox reaction [13], suggesting that the coating process was a mixed control process.Such behaviour can be interpreted as corresponding to two discrete charge

TABLE II Graphically determined values of the Randles equivalent circuit elements for the system (80 vol%) methanol—(10 vol%) ethanediol—(10 vol%) 2 M aqueous $[Ba_{0.5}Sr_{0.5}]$-EDTA

$R_\Omega \times 11^5$ ($\Omega \cdot cm^2$)	$R_{cta} \times 11^5$ ($\Omega \cdot cm^2$)	$C_{dla} \times 11^{-6}$ ($\mu F \cdot cm^{-2}$)	$R_{ctb} \times 11^5$ ($\Omega \cdot cm^2$)	$C_{dlb} \times 11^{-6}$ ($\mu F \cdot cm^{-2}$)	$\sigma \times 11^7$ ($\Omega \cdot sec^{-1/2} \cdot cm^2$)
2.1	2.65	37.7	7.03	8.89	7.02

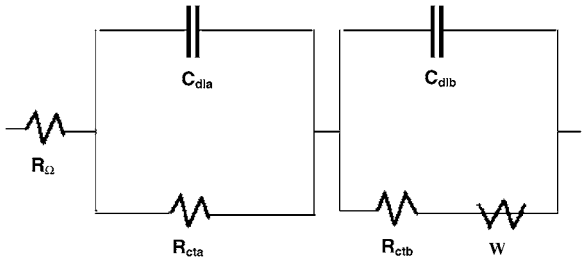

Figure 10 The equivalent Randles circuit for the complex impedance diagrams shown in Figs 8, 9 and 11.

transfer processes and diffusion control processes. A suitable equivalent circuit which can provide a consistent model for these effects is shown in Fig. 10, with calculated values for the respective circuit elements for the methanol-ethanediol (10 v%)-$[Ba_{0.5}Sr_{0.5}]$-EDTA sol (10 v%) used for the EPD process given in Table II.

As might be anticipated for the methanol media used in this study the calculated real and imaginary components of the impedance were both extremely high (of the order of 10^7 ohms cm^2) as shown in Fig. 8, whereas in contrast, the addition of the $[Ba_{0.5}Sr_{0.5}]$-EDTA produced a large reduction in these values by around two orders of magnitude. (Fig. 9)

The most probable explanation of the charge transfer phenomenon in the organic media is that the electric field resulted in some disassociation of the methanol and/or trace absorbed water in the solution to produce mobile H^+ and H_3CO^- and/or OH^- ions. The two charge transfer processes represented by the semicircular regions on the complex impedance plots represent the interaction of these anionic and cationic species with the electrodes. The linear region of the plot corresponds to diffusion control at very low AC frequencies (0.1 to 0.05 Hz) and is most probably associated with the migration of the charged species to the electrode.

The addition of aqueous $[Ba_{0.5}Sr_{0.5}]$-EDTA sol to the organic solvent dramatically increases the concentration of both water and H^+ ions present in the system, accounting for the large decrease in solution resistance, represented by the residual real component of Z' at very high frequencies (intercept on Z' axis) in Fig. 9. In comparison with the organic system shown in Fig. 8, the range of frequencies over which diffusion controlled behaviour occurs becomes much greater (below 3.5 Hz), suggesting that the mobility of the charge carrying species is reduced in this case. Most probably the complexed MY^{2-} ions are the dominant and rate limiting species in this system.

Figs 11 and 12 illustrate the effect of increasing the concentration of the $[Ba_{0.5}Sr_{0.5}]$-EDTA component and the "deposition time" in the EIS cell respectively. It can be seen that increasing the $[Ba_{0.5}Sr_{0.5}]$-EDTA concentration results in a systematic decrease in the solution and charge transfer resistances represented by the positions of the two semicircular regions. Diffusion controlled behaviour becomes increasingly significant as the concentration is increased, with diffusion control occurring only at frequencies below 0.36 Hz for 4 vol% additions of 2 M $[Ba_{0.5}Sr_{0.5}]$-EDTA with this occurring for frequencies of $<$2.5 Hz at 8 vol%, and $<$3.5 Hz at 12 vol%. The effects of increasing deposition time are somewhat different. In this case a differential effect is apparent for the first (high frequency)

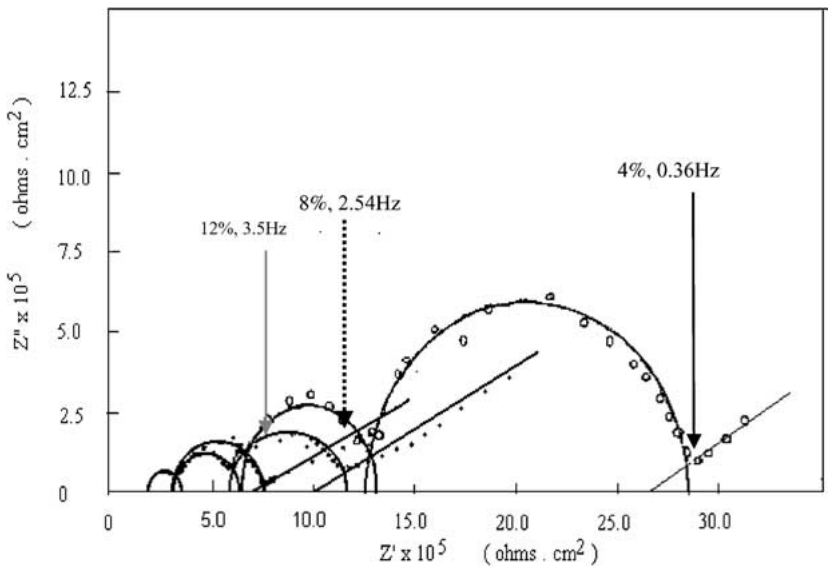

Figure 11 The complex impedance diagram for solutions of methanol-ethanediol with different concentrations of 2 M aqueous $[Ba_{0.5}Sr_{0.5}]$-EDTA (vol%).

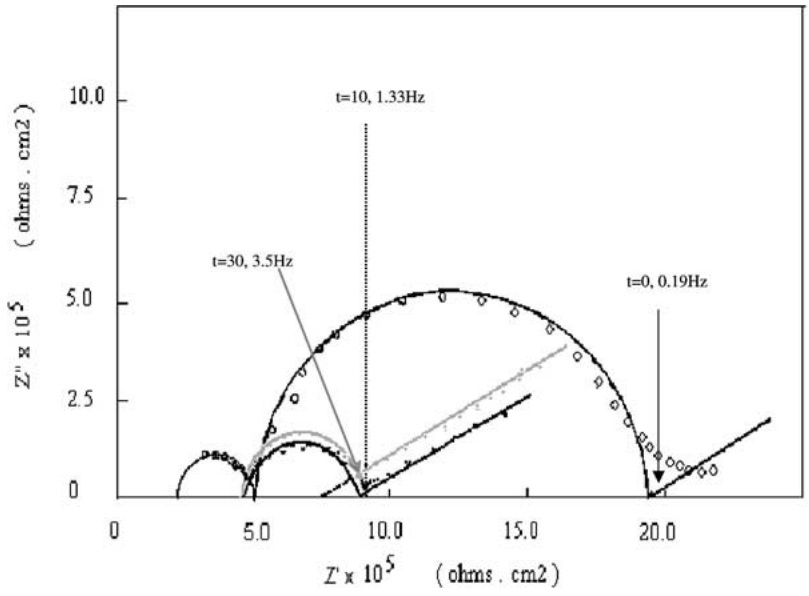

Figure 12 The complex impedance diagram obtained for (80 vol%) methanol—(10 vol%) ethanediol—(10 vol%) 2 M aqueous $[Ba_{0.5}Sr_{0.5}]$-EDTA after different deposition times (t = minutes).

charge transfer step and solution resistance, both of which are largely unaffected by time, whilst the second charge transfer step becomes more facile, indicated by the corresponding reduction in the size of the second semicircular region in the complex impedance plot. Diffusion controlled behaviour also becomes increasingly significant with increasing deposition time. In this case, diffusion controlled behaviour is only observed at frequencies lower than 0.19 Hz for initial measurements, with this value changing to frequencies <1.33 Hz after 10 minutes and <3.5 Hz after 30 minutes of deposition under the 1000 mV bias voltage conditions used in the measuring cell.

From comparison of the electrical behaviour and the observed nature of the coating formation described for the EPD process, it is probable that the above effect is associated with the gradual formation of a localised high concentration of MY^{2-} species adjacent to the anode under the action of the applied field, and the subsequent precipitation and growth of these ions as, less mobile (hence diffusion controlled) colloidal species, as illustrated in Fig. 2. This latter process is analogous to particle coagulation at the electrode in conventional EPD based on particulate sols.

The effects of increasing concentration in Fig. 11, would also seem to be consistent with the formation of less mobile species as the concentration is increased. Such an effect might be anticipated given that these higher concentration systems would be closer to their solubility limit and thus would have a greater propensity for the formation of colloidal precipitates rather than MY^{2-} species in solution.

The coating process from the aqueous organic systems thus most probably occurs by a complex process involving the transport of charged complex species to the electrode surface, the transfer of electrons at the electrode and the aggregation of the uncharged particles within the interface region followed by particle adhesion both to the anode surface and via inter-particle attractions.

4. Conclusions

1. A direct EDTA-sol electrophoretic deposition process for coating production has been developed. Adherent coatings with thickness up to 32 μm have been deposited by this process, with these coatings shrinking by around 75% on heating at 700°C but remaining crack free.

2. Aqueous systems containing Metal-EDTA complexes were unsuitable for use in EPD due to their high conductivity. However, suitably stabilised systems in organic media could be used.

3. The coatings produced by this process are highly porous, and are suitable for applications exploiting the surface properties of the coating such as catalysis or electron emission rather than as barrier coatings.

4. The coating process was investigated by electrochemical impedance spectroscopy. The results suggest that the coating process might comprise the transport of charged complex species to the electrode surface, the precipitation of these species caused by local concentration increase adjacent to the anode, followed by particle adhesion both to the anode surface and via inter-particle attractions.

References

1. B. M. WECKHUYSEN, G. MESTL, M. P. ROSYNEK, T. R. KRAWIETZ, J. F. HAW and J. H. LUSFORD, *J. Physical Chemistry* B **102**(19) (1998) 3773.
2. V. R. CHOUDHARY, B. PRABHAKAR, A. M. RAJPUT and A. S. MAMMAN, *Fuel* **77**(13) (1998) 1477.
3. G. A. HAAS, in "Methods of Experimental Physics," Vol. 4, edited by V. W. Hughes and H. L. Schultz (Academic Press, New York, 1967) p. 1.
4. P. SARKAR and P. S. NICHOLSON, *J. Amer. Ceram. Soc.* **79** (1996) 1987.
5. Z. R. ULBERG, Y. F. DEINEGA and T. J. KEMP, in "Electrophoretic Composite Coatings" (Ellis Horwood, New York, 1992) p. 11.
6. D. DE and P. S. NICHOLSON, *J. Amer. Ceram. Soc.* **82** (1999) 3031.
7. H. NISHIMORI, M. TATSUMISAGO and T. MINAMI, *J. Mater. Sci.* **31** (1996) 6529.

8. S. N. B. HODGSON, X. SHEN and F. R. SALE, *ibid*. **35** (2000) 5275.
9. J. FRANSAER, J. R. LOOS, L. DELAEY, V. D. BIEST, O. ARKENS and J. P. CELIS, *J. Appl. Phys.* **65** (1989) 3277.
10. A. GHOLINIA and F. R. SALE, *J. Therm. Anal.* **42** (1994) 733.
11. D. T. SAWYER and P. J. PAULSEN, *J. Am. Chem. Soc.* **80** (1958) 1597.
12. J. Y. CHOUDHARY, H. S. RAY and K. N. RAI, *Trans. J. Br. Ceram. Soc.* **81** (1982) 189.
13. R. GREEF, R. PEAT, L. M. PETER, D. PLETCHER and J. ROBISON, in "Electrochemistry" (Ellis Horwood, New York, 1990) p. 251.
14. P. J. GELLINGS and H. J. M. BOUWMEESTER, "The CRC Handbook of Solid State Electrochemistry" (CRC Press, Boca Raton, 1997).

Received 24 October 2000
and accepted 14 March 2002